



Contents lists available at ScienceDirect

Journal of Dermatological Science

journal homepage: [www.jdsjournal.com](http://www.jdsjournal.com)



# Bone marrow derived mesenchymal stem cells inhibit the proliferative and profibrotic phenotype of hypertrophic scar fibroblasts and keloid fibroblasts through paracrine signaling

Fengjun Fang<sup>a,b,1</sup>, Ru-Lin Huang<sup>c,1</sup>, Yongchao Zheng<sup>b</sup>, Ming Liu<sup>b</sup>, Ran Huo<sup>a,\*</sup>

<sup>a</sup> Department of Aesthetic, Plastic, and Burn Surgery, Shangdong Provincial Hospital, Shangdong University, No. 324 Jing 5 wei 7 Road, Jinan 250021, China

<sup>b</sup> Department of Plastic Surgery, People's Hospital of Jimo, No. 4 Jianmin Road, Jimo 266200, China

<sup>c</sup> Department of Plastic and Reconstructive Surgery, Shanghai Ninth People's Hospital, Shanghai Jiao Tong University School of Medicine, 639 Zhizaoju Road, Shanghai 200011, China

## ARTICLE INFO

### Article history:

Received 19 September 2015

Received in revised form 16 February 2016

Accepted 3 March 2016

### Keywords:

BMSC

Hypertrophic scar

Keloid

Profibrotic

Proliferative

## ABSTRACT

**Background:** Hypertrophic scars and keloids, characterized by over-proliferation of fibroblasts and aberrant formation of the extracellular matrix (ECM), are considered fibrotic diseases. Accumulating evidence indicates that mesenchymal stem cells (MSCs) promote scar-free wound healing and inhibit fibrotic tissue formation, making them a potentially effective therapeutic treatment for hypertrophic scars and keloids.

**Objective:** To investigate the paracrine effects of bone marrow derived MSCs (BMSCs) on the biological behavior of hypertrophic scar fibroblasts (HSFs) and keloid fibroblasts (KFs).

**Methods:** Proliferative and profibrotic phenotype changes of the fibroblasts were analyzed by immunofluorescence staining, in-cell western blot, and real-time PCR.

**Results:** BMSC-conditioned medium inhibited HSF and KF proliferation and migration, but did not induce apoptosis. Interestingly, normal skin fibroblast-conditioned medium exhibited no inhibitory effects on HSF or KF proliferation and migration. Furthermore, BMSC-conditioned medium significantly decreased expression of profibrotic genes, including connective tissue growth factor, plasminogen activator inhibitor-1, transforming growth factor- $\beta_1$ , and transforming growth factor- $\beta_2$ , in HSFs and KFs at both transcriptional and translational levels. In contrast, the expression of antifibrotic genes, such as transforming growth factor- $\beta_3$  and decorin, was substantially enhanced under the same culture conditions. Finally, we observed that BMSC-conditioned medium suppressed the ECM synthesis in HSFs and KFs, as indicated by decreased expression of collagen I and fibronectin and low levels of hydroxyproline in cell culture supernatant.

**Conclusion:** These findings suggest that BMSCs attenuate the proliferative and profibrotic phenotype associated with HSFs and KFs and inhibit ECM synthesis through a paracrine signaling mechanism.

© 2016 Published by Elsevier Ireland Ltd on behalf of Japanese Society for Investigative Dermatology.

## 1. Introduction

Pathological scarring is a response to wound healing in postnatal mammalian skin that can be considered a fibroproliferative disorder (FPD) [1]. Hypertrophic scars, especially keloids, are characterized by fibroblast over-proliferation and excessive formation of the extracellular matrix (ECM) that appears to be mainly driven by fibroblasts [2]. However, keloids are distinguishable from hypertrophic scars. A keloid is a benign dermal

overgrowth that extends beyond the boundaries of the original wound, does not regress spontaneously, and commonly recurs after surgical excision. By contrast, hypertrophic scars remain within the boundaries of the original wound, frequently regress spontaneously, and rarely recur after surgical excision [3,4]. Hypertrophic scarring and keloid formation severely impair the quality of life by causing cosmetic and functional deformities, discomfort, and psychological stress. Although many therapeutic approaches, such as surgical excision, corticosteroid injection, compression therapy, and laser therapy, have been applied to hypertrophic scars and keloids, there remains no satisfactory treatment to completely erase scars in humans. Thus, new therapies and novel strategies are required for the treatment of hypertrophic scars and keloids.

\* Corresponding author.

E-mail address: [huoran2015@126.com](mailto:huoran2015@126.com) (R. Huo).

<sup>1</sup> These authors contributed equally to this work.

Very little is known about keloid and hypertrophic scar pathogenesis, which contributes to the lack of proper treatment strategies. Hypertrophic scars and keloids are consequences of cutaneous wound healing and share several pathobiological features with other fibrotic diseases, such as scleroderma [5]. There is increasing evidence that mesenchymal stem cells (MSCs) exhibit a number of trophic functions that promote scar-free wound healing and inhibit fibrotic tissue formation [6–9]. These functions include modulation of macrophage and T-cell function during wound healing, neutralization of reactive oxygen species in the wound, production of antifibrotic factors, enhancement of dermal fibroblast functions, promotion of angiogenesis and vascular stability, and differentiation into dermal cell types [7,9]. As a result, MSCs have been considered and tested as candidates for cellular therapy in FPDs. Indeed, preclinical and clinical trials have shown the ability of MSCs, such as bone marrow derived mesenchymal stem cells (BMSCs) [10,11], umbilical cord-derived mesenchymal stem cells [12], plate-derived mesenchymal stem cells [6], and adipose derived stem cells [13], to improve outcomes in various fibrotic diseases. Additionally, umbilical cord-derived Wharton's Jelly derived mesenchymal stem cells (WJ-MSCs) [14] have been used to improve wound healing [15]. Treatment of murine skin defects with human BMSCs (hBMSCs) resulted in scar-free healing in 14 days [16]. The hBMSCs secrete a variety of cytokines and growth factors, including hepatocyte growth factor and IL-10, having antifibrotic properties. Furthermore, nearly 30 clinical trials are currently registered worldwide for evaluating MSC therapy for fibrosis (<http://clinicaltrials.gov>) [9]. Accumulating evidence suggests that paracrine signaling, the secretion of trophic or immunomodulatory factors, or secretome may represent the most pivotal components of the mechanism accounting for the effects of MSCs [17–19].

Although it is unlikely that isolated MSCs can replicate the complete mechanisms of scar-free wound healing that occur in fetal dermal tissues, they may still be able to re-initiate or promote some aspects of the healing process, such as inhibition of fibroblast proliferation and ECM deposition. In this study, we tested *in vitro* the effects of BMSC paracrine signaling on the proliferative and profibrotic phenotypes associated with hypertrophic scar fibroblasts (HSFs) and keloid fibroblasts (KFs). We found that BMSC-conditioned medium inhibited cell proliferation and migration and attenuated the profibrotic phenotype and collagen synthesis associated with HSFs and KFs. Our findings suggest that BMSCs are potential therapeutic agents for the treatment of hypertrophic scars and keloids.

## 2. Materials and methods

### 2.1. Patients and tissue samples

Keloid, hypertrophic scar, and mature scar tissues were harvested at the time of surgery from patients confirmed to have clinical and pathological evidence of these conditions and who had not yet received scar treatment. Only clinically typical samples were included in this study. Additionally, normal skin samples were obtained from patients during unrelated surgical operations (Table 1). The study was approved by the Medical and Ethics Committee of our hospital. All persons recruited gave full verbal and written consent to take part in the study.

### 2.2. Isolation and culture of cells

Fibroblast cultures were established from tissue specimens that were processed within 6 h of post-surgical excision as previously described [20]. Briefly, the specimens were sectioned into 2–3 cm pieces and repeatedly washed in sterile Dulbecco's Modified

**Table 1**  
Patient epidemiological data.

Subject	Age(y)	Sex	Region	Age (mo)
<b>Keloid</b>				
1	18	F	Earlobe	14
2	31	F	Earlobe	32
3	39	M	Shoulder	21
4	22	F	Sternum	16
5	28	F	Earlobe	8
6	35	F	Sternum	24
7	33	F	Sternum	42
8	25	M	Earlobe	10
<b>Hypertrophic scar</b>				
1	22	F	Shoulder	12
2	34	F	Neck	8
3	32	M	Neck	15
4	53	F	Face	14
5	24	M	Cheek	5
6	19	M	Back	9
7	13	M	Scalp	96
8	38	F	Shoulder	11
9	42	M	Abdomen	10
10	34	F	Abdomen	8
<b>Mature scar</b>				
1	15	F	Face	16
2	45	F	Arm	60
3	27	M	Arm	18
4	32	F	Abdomen	22
5	37	M	Abdomen	24
6	52	M	Face	32
<b>Normal skin</b>				
1	38	M	Neck	N/A
2	23	M	Abdomen	N/A
3	43	F	Eyelid	N/A
4	25	F	Back	N/A
5	32	F	Shoulder	N/A
6	35	M	Breast	N/A
7	52	F	Breast	N/A

Eagle's Medium (DMEM; Gibco, NY, USA) supplemented with 100 U/mL penicillin, 0.1 g/mL streptomycin, and 1.25 ng/mL Fungizone (Gibco). The specimens were then exposed to 3 mg/mL Dispase II (Invitrogen, CA, USA) in DMEM overnight at 4°C. Following overnight incubation, the epidermis was removed and the dermis minced into small pieces (1 mm<sup>3</sup>). The pieces were placed in 4 mg/mL collagenase, type I (Sigma-Aldrich, MO, USA) and incubated at 37°C in 5% CO<sub>2</sub> atmosphere for 2 h. After enzymatic digestion, the cell suspension was centrifuged at 300g for 5 min and the cell pellet resuspended in DMEM supplemented with 10% fetal bovine serum (FBS; Gibco). The cell suspension was then filtered through a 70 µm cell strainer (BD Biosciences, CA, USA), and centrifuged at 300g for 5 min. The supernatant was discarded and the cells were cultured in 100 mm plastic tissue culture Petri dishes (BD Biosciences). Once confluent normal skin fibroblasts (NFs), mature scar fibroblasts (MSFs), HSFs, and KFs were established as monolayer cultures, cell passaging was carried out using 0.25% trypsin (Gibco).

Human bone marrow was aspirated from the iliac crest of four healthy male and female donors, aged 23–46 years, following approval of the Institutional Review Board. Written informed consent was obtained from all patients. The hBMSCs were isolated based on their capacity to adhere to tissue culture plastic, and the isolated cells from each donor were maintained separately. The immunologic phenotypes of hBMSCs were positive for CD29 (98.32%), CD44 (75.45%), and CD90 (97.57), but negative for CD11b (1.32%), CD34 (0.75%), and CD45 (0.64%) (Supplementary Fig. S1A). We also demonstrated that the hBMSCs could differentiation into

osteoblasts and adipocytes (Supplementary Fig. S1B). Only passage 2 hBMSCs were used in this study.

### 2.3. Preparation of BMSC- and NF-conditioned medium

The hBMSCs and NFs at passage 2 were grown to 80% confluence in DMEM supplemented with 10% FBS, and the culture media separated after 72 h and designated as BMSC- or NF-conditioned medium. The conditioned media were stored at  $-80^{\circ}\text{C}$  until required, then thawed overnight ( $4^{\circ}\text{C}$ ) and subsequently filter-sterilized through a 0.22 mm Millex-GP syringe filter (Millipore, Billerica, MA, USA). The pH and osmolality of the media were standardized before use in experiments. Both BMSC- and NF-conditioned medium were diluted 1:1 (v/v) with DMEM supplemented with 10% FBS and used as 50% BMSC- and 50% NF-conditioned medium for the following experiments. PBS diluted 1:1 (v/v) with DMEM supplemented with 10% FBS (PBS + complete medium) was used as control medium.

### 2.4. Treatment of target fibroblasts with BMSC- and NF-conditioned medium

Adherent NFs, MSFs, HSFs, and KFs cultures were separately treated with PBS + complete medium, BMSC-conditioned medium, or NF-conditioned medium. All dishes were refreshed every 2 days. Cells were subjected to comparative analyses, including cell proliferation (Cell Counting Kit 8, CCK-8 assay), cell cycle behavior (flow cytometry), scratch-wound assay, collagen I synthesis (hydroxyproline content detection), protein expression (immunofluorescence staining and In-cell western blotting), and gene expression profiles (real-time PCR).

### 2.5. Cellular proliferation

The CCK-8 (Dojindo, Shanghai, China) assay was used to determine the extent of fibroblasts proliferation. Fibroblasts were seeded in 96-well plates at an initial density of 4000 cells/well. After treatment with PBS + complete medium, BMSC-conditioned medium, or NF-conditioned medium, the CCK-8 reagent was added for an incubation period of 2 h at  $37^{\circ}\text{C}$ . The absorption rate and the reference wavelength were measured at 450 nm and 600 nm, respectively.

### 2.6. Terminal dUTP nick end labeling (TUNEL) assay

Fibroblasts were seeded and cultured in 24-well plates at a density of  $1 \times 10^5$  cells/well for 8 h. Cells were then exposed to PBS + complete medium, BMSC-conditioned medium, or NF-conditioned medium for 48 h. A TUNEL apoptosis kit (Beyotime, Lianyungang, China) was used according to manufacturer instructions. Three images per well were taken using an Apotome Axiovert fluorescent imaging system (Zeiss, Göttingen, Germany) at  $10\times$  magnification. Quantification was performed by counting the number of TUNEL- and 4',6-diamidino-2-phenylindole (DAPI)-positive nuclei, denoting viable or apoptotic, respectively.

### 2.7. Scratch-wound assay

Fibroblasts were first seeded at a density of  $1 \times 10^6$  cells/60 mm dish and monolayers established after 48-h culture using complete medium. Uniform linear scratches were formed on the fibroblast monolayers vertically from top to bottom at the midline using a 2 mL graduated serological pipette. The cell debris was washed away with PBS and the medium in the dishes changed to PBS + DMEM, BMSC-conditioned medium (FBS-free), or NF-conditioned medium (FBS-free). The dishes were incubated at  $37^{\circ}\text{C}$  in 5%

$\text{CO}_2$  atmosphere for 24 h. Cell migration from the edge of the scratch was monitored regularly and digitized images of at least five random fields within the scratched area were taken using inverted phase contrast optics after 24 h treatment. The number of cells that had migrated into the scratched area was counted with a standardized scratch area for each image. Three replicates were undertaken for each assay.

### 2.8. Hydroxyproline content detection

The determination of hydroxyproline content in the cell supernatant was carried out using a hydroxyproline alkali hydrolysis kit (Nanjing Jiancheng Bioengineering Institute, Nanjing, China) according to manufacturer instructions. Briefly, after treatments, culture medium was collected, centrifuged at 1200g for 15 min, the supernatant collected, and 1 mL chloramine T solution added to the supernatant samples and to hydroxyproline standards. Following incubation for 20 min at room temperature, 1 mL hydroxyproline developer ( $\beta$ -dimethylaminobenzaldehyde solution) was added to the samples and the standards. The absorbance of the solution was measured at a wavelength of 550 nm; and the levels of hydroxyproline/mL in the supernatant were calculated using the standard curve generated by the serial dilutions of the hydroxyproline standards.

### 2.9. In-cell western blot

Fibroblasts in 96-well plates were treated with conditioned media for 96 h and fixed in 4% paraformaldehyde for 20 min at room temperature. Cells were washed three times with PBS, permeabilized with 0.1% Triton X-100, and blocked with Odyssey blocking buffer (LI-COR Biosciences, Cambridge, UK) for 2 h at room temperature. Primary antibodies used in this study included those against collagen type I, fibronectin, transforming growth factor (TGF)- $\beta_1$ , TGF- $\beta_2$ , TGF- $\beta_3$ , connective tissue growth factor (CTGF), plasminogen activator inhibitor-1 (PAI-1), and decorin (Table 2). A mouse or rabbit anti- $\beta$ -tubulin primary antibody (Table 2) was also used to simultaneously stain each well in order to measure housekeeping gene expression. All primary antibody

**Table 2**

List of antibodies used in this study.

Antibody	Species Raised	Isotype	Dilution	Product Code	Source
Collagen I	Rabbit polyclonal	IgG	WB: 1: 1000 IF: 1: 100	ab34710	Abcam
Fibronectin	Mouse monoclonal	IgG	WB: 1: 400 IF: 1: 100	ab6328	Abcam
PAI-1	Rabbit polyclonal	IgG	WB: 1: 500 IF: 1: 50	ab66705	Abcam
CTGF	Rabbit polyclonal	IgG	WB: 1: 1000 IF: 1: 100	ab6992	Abcam
TGF- $\beta_1$	Mouse polyclonal	IgG1	WB: 1: 500 IF: 1: 100	ab64715	Abcam
TGF- $\beta_2$	Rabbit polyclonal	IgG	WB: 1: 1000 IF: 1: 200	ab66045	Abcam
TGF- $\beta_3$	Rabbit polyclonal	IgG	WB: 1: 500 IF: 1: 50	ab15537	Abcam
Decorin	Mouse monoclonal	IgG2b	WB: 1: 500 IF: 1: 50	ab54728	Abcam
$\beta$ -tubulin	Rabbit monoclonal	IgG	WB: 1: 1000	2148	CST
$\beta$ -tubulin	Mouse monoclonal	IgG	WB: 1: 500	ab40862	Abcam

Abbreviations: CST—Cell Signaling Technology; IF— immunofluorescence; WB— western blot.

**Table 3**  
List of oligonucleotides used for quantitative real-time PCR.

Target gene	Sequence	Reference
Collagen I	F: 5'-AGTGGTTTGATGGTGCCAA-3' R: 5'-GCACCATCATTTCACGAGC-3'	NM_000088.3
Fibronectin	F: 5'-ACAAGCATGTCTCTGCGCA-3' R: 5'-TCAGGAACTCCAGGGTGA-3'	NM_212482.1
PAI-1	F: 5'-AGAGCGCTGTCAAGAAGACC-3' R: 5'-AGTTCTCAGAGGTGCCTTGC-3'	NM_000602.4
CTGF	F: 5'-GTTTGGCCAGACCAACTA-3' R: 5'-GGCTCTGCTTCTAGCCTG-3'	NM_001901.2
TGF- $\beta_1$	F: 5'-ATGAGAGAGAGACTGCGGAT-3' R: 5'-TAGTGTTCCTCCACTGGTCCC-3'	NM_000660.5
TGF- $\beta_2$	F: 5'-CTCCGAAATGCCATCCCGC-3' R: 5'-GCTCAATCCGTGTTCAGGC-3'	NM_003238.3
TGF- $\beta_3$	F: 5'-CGTGCCGTGAAGTGGCTTC-3' R: 5'-AATCATCCACTCAGACGCC-3'	NM_003239.3
Decorin	F: 5'-GACAGACCAAGCAGCAAAA-3' R: 5'-CTGGCTCATCCAGCAAGAT-3'	NM_133503.2
GAPDH	F: 5'-AATGGGCGAGCCGTAGGAAA-3' R: 5'-GCGCCCAATACGACCAATC-3'	NM_001256799.2

Abbreviations: F—forward primer; R—reverse primer.

incubations were carried out overnight at 4 °C. All rabbit primary antibodies were stained with IRDye 800CW donkey anti-rabbit secondary antibody (Li-COR Biosciences), and the mouse or rabbit  $\beta$ -tubulin primary antibody was stained with anti-rabbit or anti-mouse IRDye 680LT IgG (Li-COR Biosciences). After staining with both primary and secondary antibodies, the plates were imaged using an Odyssey infrared scanner (Li-COR Biosciences) to visualize the fluorescent dyes at their respective wavelengths (800 nm for IRDye 800CW and 700 nm for IRDye 680LT). Protein levels were normalized relative to  $\beta$ -tubulin expression (800 nm/700 nm ratio) from each cell-media combination. Data were acquired using the Odyssey software (Li-COR Biosciences), and were exported and analyzed in Excel (Microsoft Corp., Reading, UK).

## 2.10. Immunofluorescence staining

Cells were washed with PBS, fixed with 4% paraformaldehyde, and permeabilized using 0.1% Triton X-100. The cells were blocked with 5% goat serum for 60 min and then immunostained using primary antibodies against collagen I, fibronectin, PAI-1, TGF- $\beta_1$ , TGF- $\beta_2$ , TGF- $\beta_3$ , decorin, and CTGF (Table 2), followed by incubation with goat anti-rabbit or goat anti-mouse IgG Alexa Fluor-488-conjugated secondary antibodies (1:200, Invitrogen) and phalloidin (Sigma-Aldrich). Prior to examination, the samples were covered with anti-fade reagent (Cell Signaling Technology, MA, USA).

## 2.11. RNA extraction, cDNA synthesis, and real-time PCR

Cells were washed with PBS and lysed with TRIzol reagent (Invitrogen) according to manufacturer protocol. Then, 2  $\mu$ g total RNA was used for reverse transcription, and the product used for real-time PCR. The expression levels of genes were quantified using an ABI 7500 Real-Time PCR System (ThermoFisher Scientific, MA, USA). PCR primers were designed based on sequences from the corresponding genes (Table 3). All PCR amplifications were performed using an initial denaturation program of 95 °C for 30 s, followed by 40 cycles of 95 °C for 5 s and 60 °C for 34 s. Melting curve analysis was performed at 95 °C for 15 s and 60 °C for 60 s.

## 2.12. Statistical analysis

The data are expressed as the mean  $\pm$  SD of at least three independent experiments. One-way analysis of variance (ANOVA) test and Tukey's post-hoc test for multiple comparisons were used to determine significance between experimental groups. Student *t* test was used to determine significance between two groups. A *p* < 0.05 was considered statistically significant. SPSS statistics version 20 (IBM Corp., NY, USA) was used for statistical analysis.

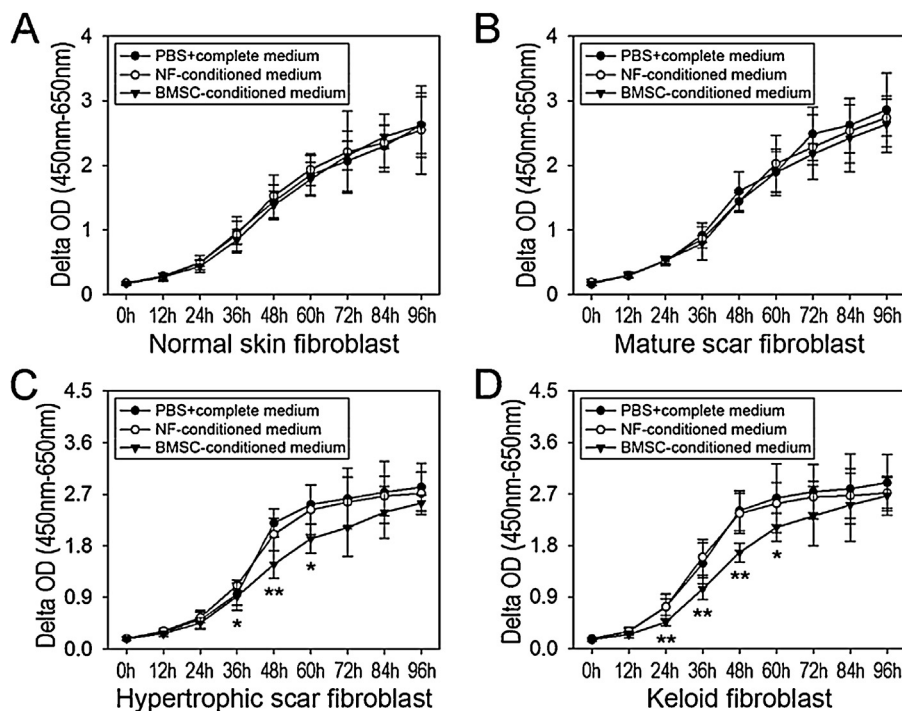


**Fig. 1.** BMSC-conditioned medium inhibits HSF and KF proliferation.

(A) NFs, (B) MSFs, (C) HSFs, and (D) KFs were cultured in PBS+complete medium, NF-conditioned medium, or BMSC-conditioned medium for 96 h. Cell viability was determined by CCK-8 assay every 12 h and compared with untreated samples. (mean  $\pm$  SD, *n* = 6, ANOVA test: \**p* < 0.05, \*\**p* < 0.01, compared with the indicated NF-conditioned medium-treated cells)



### 3. Results

#### 3.1. BMSC-conditioned medium inhibits proliferation and does not induce apoptosis in HSFs and KFs

The HSF and KF cultures exposed to BMSC-conditioned medium or NF-conditioned medium displayed inhibited cell growth relative to PBS+complete medium treated controls. As shown in Fig. 1A and B, NF-conditioned medium and BMSC-conditioned medium did not change NF or MSF proliferation rates in the 96-h cell culture relative to NFs and MSFs grown in the presence of PBS+complete medium. However, proliferation of HSFs (Fig. 1C) and KFs (Fig. 1D) decreased significantly when cultured in the presence of BMSC-conditioned medium for 24–60 h as compared with NF-conditioned medium-treated fibroblasts. In contrast, NF-conditioned medium had no effect on NF and MSF proliferation at those time points.

To further investigate the impact of BMSC-conditioned medium on NFs, MSFs, HSFs, and KFs, TUNEL assay were performed (Fig. 2A). Although the number of DAPI-positive HSFs and KFs increased after 48-h incubation with BMSC-conditioned medium relative to NF-conditioned medium-treated HSFs and KFs (Fig. 2B), no clear increase in the percentage of TUNEL-positive HSFs or KFs was observed (Fig. 2C). These results indicate that BMSC-conditioned treatment does not induce apoptosis.

#### 3.2. BMSC-conditioned medium slows HSF and KF cell migration

Representative results from the scratch-test assay for the NFs, MSFs, HSFs, and KFs cultured in either NF- or BMSC-conditioned medium are shown in Fig. 3A. After 24-h culture in complete medium, the fibroblasts were confluent. Fibroblast monolayers were then scratched and treated as previously described in Materials and methods. NFs, MSFs, HSFs, and KFs cultured in the

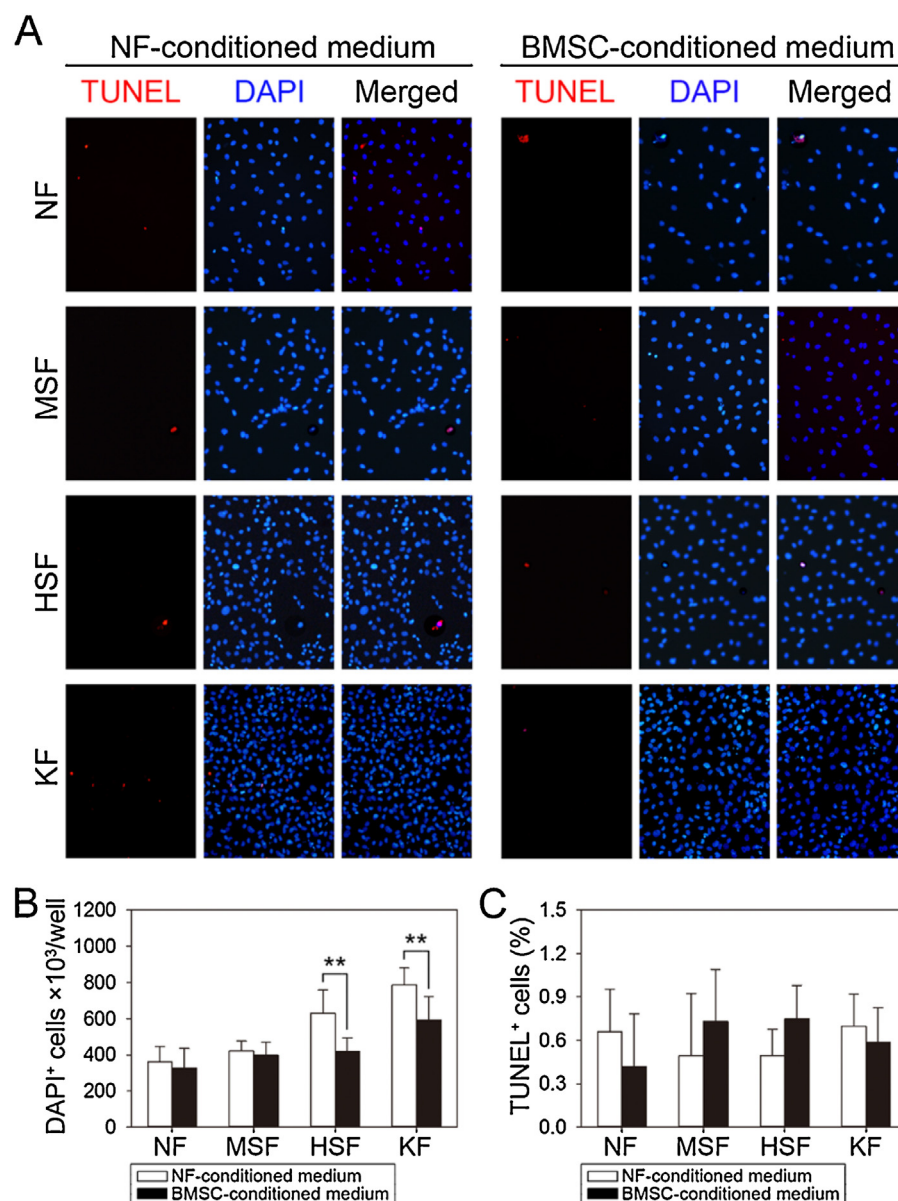


**Fig. 2.** BMSC-conditioned medium does not induce apoptosis in HSFs or KFs.

NFs, MSFs, HSFs, and KFs were cultured in NF-conditioned medium or BMSC-conditioned medium for 48 h. (A) TUNEL- and DAPI-staining were performed to determine viability. (B) The number of DAPI positive cells/cm<sup>2</sup>. (C) The percentage of TUNEL-positive cells/well. (mean ± SD, n = 5, Student t-test, \*p < 0.05, \*\*p < 0.01, compared with the indicated NF-conditioned medium-treated cells)

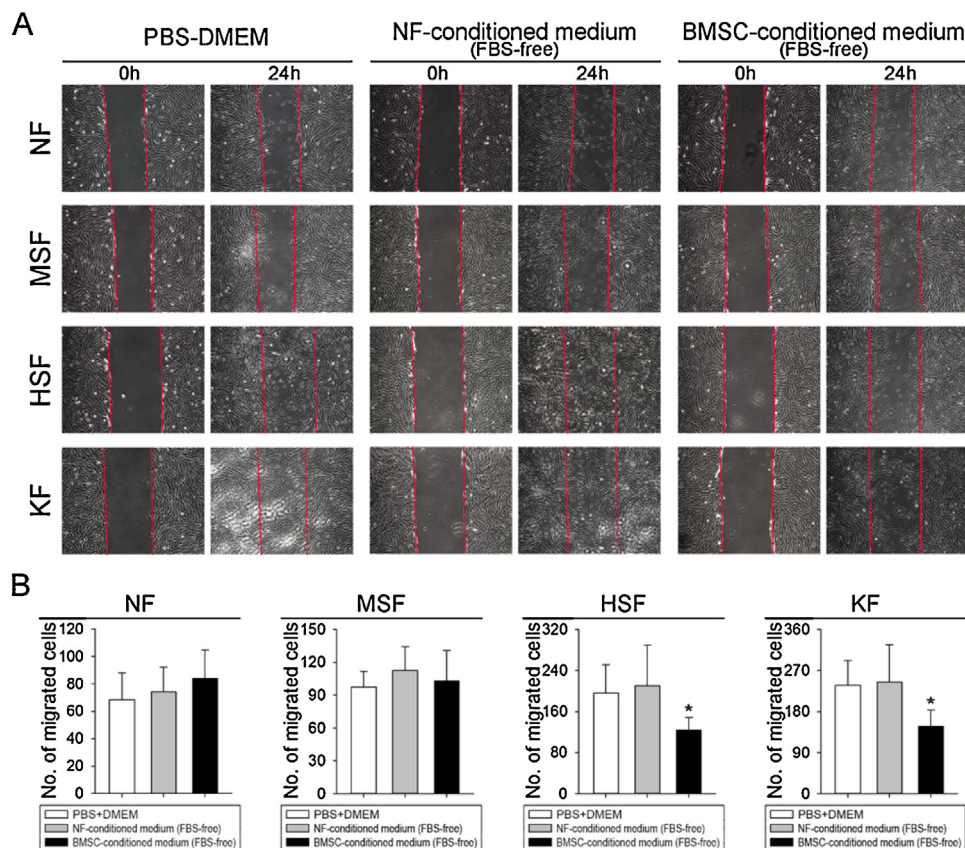


**Fig. 3.** BMSC-conditioned medium slows HSF and KF migration. NFs, MSFs, HSFs, and KFs were cultured in DMEM supplemented with 10% FBS for 48 h. When the cells reached confluence, a scratch was formed and the cells were treated with PBS + DMEM, NF-conditioned medium (FBS-free), or BMSC-conditioned medium (FBS-free) for 24 h. (A) Scratch wound assays were evaluated by digital images and (B) the number of the cells migrating into the scratch area were counted. (mean  $\pm$  SD,  $n = 5$ , Student  $t$ -test, \* $p < 0.05$ , compared with the indicated NF-conditioned medium-treated cells).

presence of NF-conditioned medium (FBS-free) exhibited no changes in cell migration relative to those cultured in PBS + DMEM. Furthermore, the numbers of NFs and MSFs that migrated from the scratch edges showed no variation between those cultured in NF-conditioned medium (FBS-free) or BMSC-conditioned medium (FBS-free). The HSFs and KFs cultured in the NF-conditioned medium (FBS-free) displayed migration into the scratch wound that completely covered the vacant areas within 24 h, while HSFs and KFs cultured in BMSC-conditioned medium (FBS-free) displayed limited migration with incomplete coverage of the scratched areas over the same time period (Fig. 3B). These data suggest that the BMSC-conditioned medium attenuates HSF and KF cell migration.

### 3.3. BMSC-conditioned medium treatment attenuates the profibrotic phenotype associated with HSFs and KFs

Hypertrophic scars and keloids are considered to be fibrotic diseases characterized by abnormal accumulation of ECM components and expression of profibrotic genes. Therefore, we analyzed expression levels of profibrotic genes in order to test the impact of the two types of conditioned media on the profibrotic phenotypes associated with HSFs and KFs. In our culture conditions, NF- and BMSC-conditioned medium did not affect the expression levels of CTGF, PAI-1, TGF- $\beta_1$ , and TGF- $\beta_2$  in NFs and MSFs. However, BMSC-conditioned medium treatment significantly decreased expression of CTGF, PAI-1, TGF- $\beta_1$ , and TGF- $\beta_2$  genes in HSFs and KFs. Interestingly, these cells maintained high expression levels of these genes after 48-h treatment with NF-conditioned medium

(Fig. 4A–D). Similar expression profiles for these profibrotic genes were observed at the protein level using an In-cell western blot (Fig. 4E–H) and immunofluorescence staining (Fig. 5). These results suggest that BMSC-conditioned medium inhibits the profibrotic phenotypes associated with HSFs and KFs, but does not affect NFs or MSFs.

### 3.4. BMSC-conditioned medium increases antifibrotic gene expression at the transcriptional and translational levels in HSFs and KFs

As shown in Fig. 6, expression of the antifibrotic factors TGF- $\beta_3$  and decorin at the transcriptional (Fig. 6A and B) and translational levels (Fig. 6C and D) was significantly higher in NFs as compared with HSFs or KFs under NF-conditioned medium culture conditions. However, after 48-h treatment with BMSC-conditioned medium, TGF- $\beta_3$  and decorin transcription and translation levels increased. In contrast, BMSC-conditioned medium treatment did not affect TGF- $\beta_3$  and decorin levels in NFs or MSFs (Fig. 6A–F). These results indicate that BMSC-conditioned medium may exhibit a protective role against hypertrophic scarring and keloid formation.

### 3.5. BMSC-conditioned medium inhibits ECM synthesis in HSF and KF cultures

Collagen I and fibronectin are two major ECM components that are upregulated in hypertrophic scars and keloids. To determine the paracrine effect of BMSC-conditioned medium on ECM synthesis, expression of collagen I and fibronectin at the

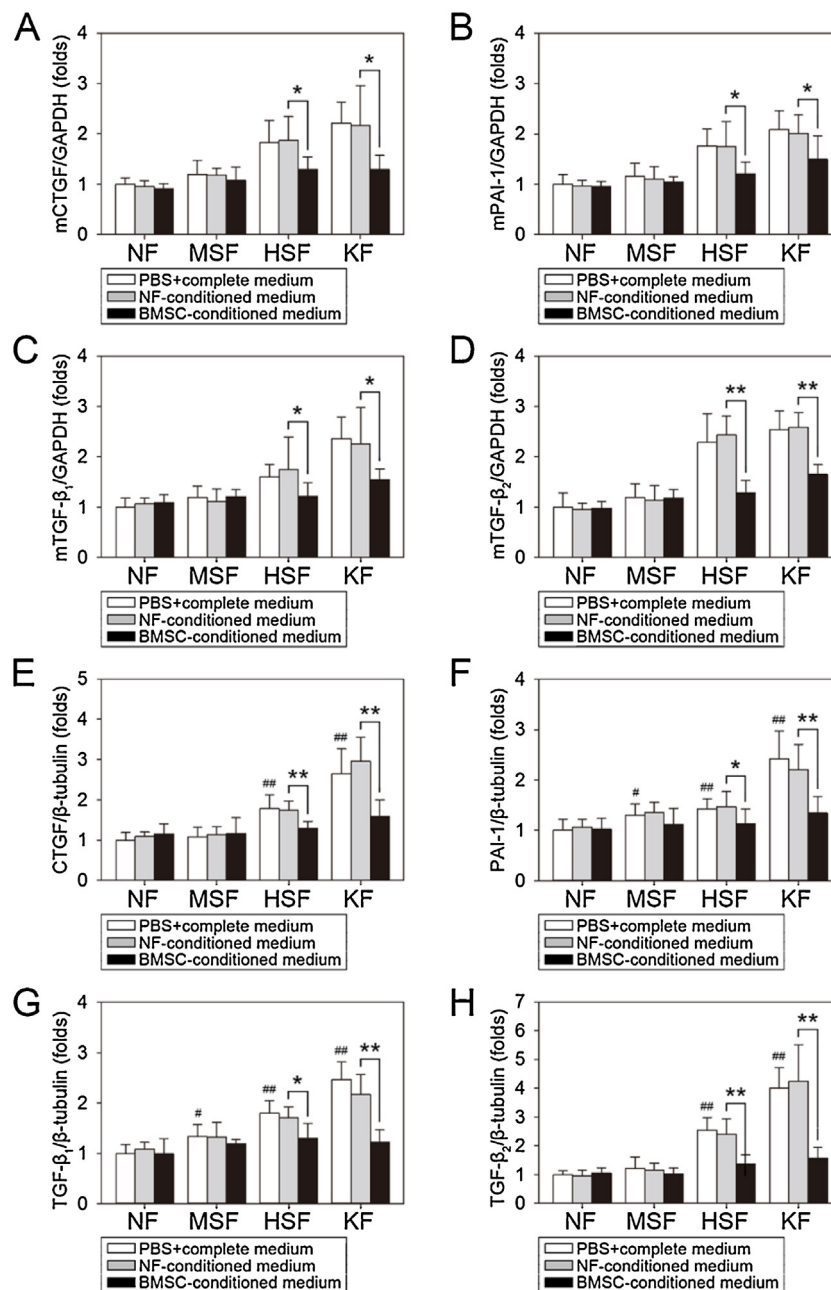


**Fig. 4.** BMSC-conditioned medium treatment attenuates the profibrotic phenotype of HSFs and KFs.

NFs, MSFs, HSFs, and KFs were cultured with PBS + complete medium, NF-conditioned medium, or BMSC-conditioned medium for 48 h, and then subjected to real-time PCR and In-cell western blot. (A–D) Quantification of (A) CTGF, (B) PAI-1, (C) TGF-β<sub>1</sub>, and (D) TGF-β<sub>2</sub> gene expression, normalized to GAPDH expression. (E–H) Quantification of (E) CTGF, (F) PAI-1, (G) TGF-β<sub>1</sub>, and (H) TGF-β<sub>2</sub> protein levels, normalized to β-tubulin expression (mean ± SD, n = 3, Student *t*-test, \**p* < 0.05, \*\**p* < 0.01, compared with the indicated NF-conditioned medium-treated cells; #*p* < 0.05, ##*p* < 0.01, compared with the NFs).

transcriptional and translational levels was analyzed by real-time PCR and In-cell western blot, respectively. Under our culture conditions, we found that BMSC-conditioned medium decreased collagen I and fibronectin expression at both the transcriptional level and translational levels (Fig. 7A–D and F–G).

Hydroxyproline is a prominent component of collagen and accounts for 13.4% of the amino acids in collagen tissue. The hydroxyproline content of tissue could, therefore, reflect collagen formation and indicate the amount and consistency of scar tissue [21]. In this study, BMSC-conditioned medium did not affect the hydroxyproline concentration in cultures of NFs and MSFs. However, hydroxyproline content significantly decreased from

6.05 mg/mL to 4.10 mg/mL in HSF cell culture supernatant, and from 7.79 mg/mL to 4.36 mg/mL in KF culture supernatant (Fig. 7E).

#### 4. Discussion

Preclinical and clinical studies have demonstrated that MSCs exhibit therapeutic functions that promote wound healing and limit scar formation, making them an attractive therapeutic candidate for treating hypertrophic scars and keloids. For example, transplantation of caprine WJ-MSCs diminishes scarring in goats [22] and treatment of human keloid fibroblasts with human WJ-MSC-conditioned medium or lysate decreases cell proliferation



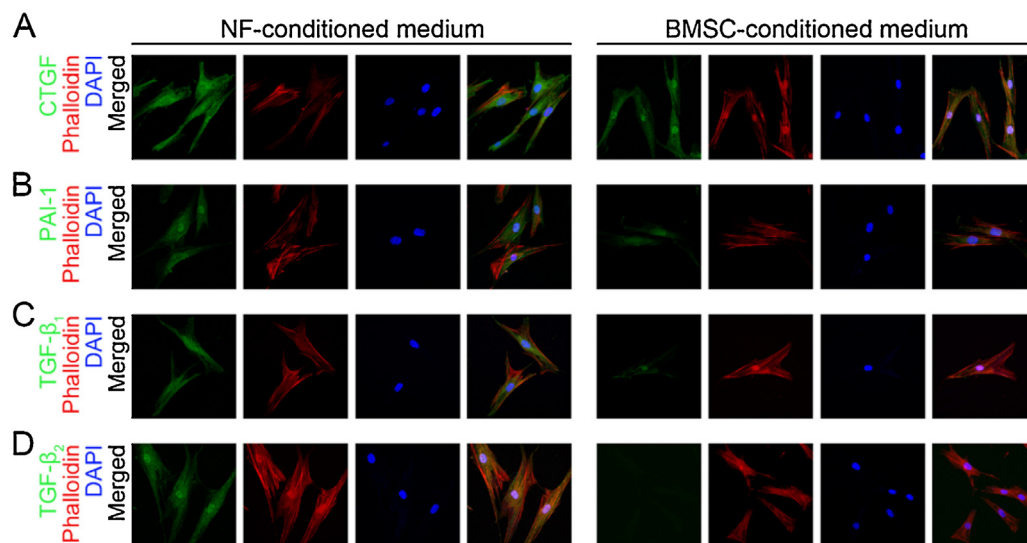


**Fig. 5.** BMSC-conditioned medium treatment inhibits profibrotic protein expression in KFs. KFs were cultured with NF-conditioned medium or BMSC-conditioned medium for 48 h, and then subjected to immunofluorescence staining to detect (A) CTGF, (B) PAI-1, (C) TGF- $\beta_1$ , and (D) TGF- $\beta_2$  protein expression. Original magnification: 200X. ( $n=3$ )

and migration in vitro [23]. However, there are currently no reports of using hBMSCs to treat hypertrophic scars and/or keloids. In this study, we hypothesized that hBMSCs may affect the biological behavior of keloid and hypertrophic scar. Then, we used the cell

culture supernatant of hBMSCs to treat the NFs, MSFs, HSFs, and KFs. The results show that the BMSC-conditioned medium inhibit the proliferation and profibrotic phenotype of HSFs and KFs. The paracrine signaling of hBMSCs, such as the release of

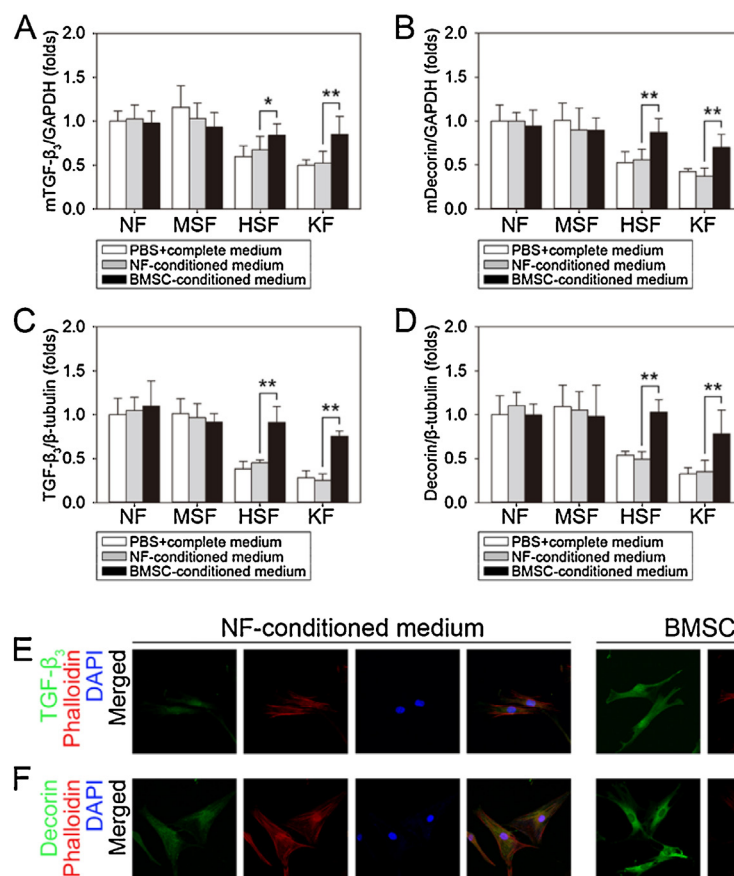


**Fig. 6.** BMSC-conditioned medium increases antifibrotic gene expression at the transcriptional and translational levels in HSFs and KFs. HSFs and KFs were cultured in PBS + complete medium, NF-conditioned medium, or BMSC-conditioned medium for 48 h, and then subjected to real-time PCR, in-cell western assay, and immunofluorescence staining. (A and B) Quantification of (A) TGF- $\beta_3$  and (B) decorin gene expression, normalized to GAPDH expression. (C and D) Quantification of (C) TGF- $\beta_3$  and (D) decorin protein levels, normalized to  $\beta$ -tubulin levels; (E and F) Immunofluorescence staining for (E) TGF- $\beta_3$  and (F) decorin in KFs. Magnification: 200 $\times$ . (mean  $\pm$  SD,  $n=3$ , Student  $t$ -test, \* $p < 0.05$ , \*\* $p < 0.01$ , compared with the indicated NF-conditioned medium-treated cells)



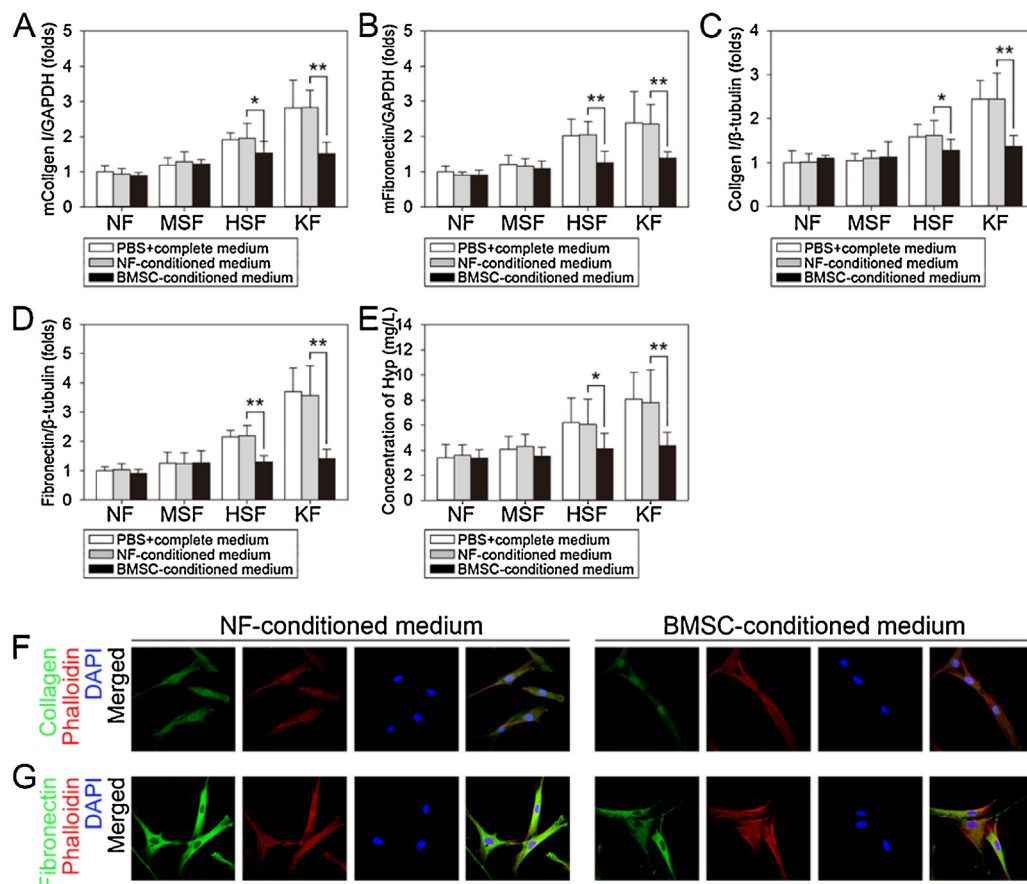


**Fig. 7.** BMSC-conditioned medium inhibits ECM synthesis in HSF and KF cultures. NFs, MSFs, HSFs, and KFs were cultured with PBS + complete medium, NF-conditioned medium, or BMSC-conditioned medium for 48 h, and then subjected to real-time PCR, In-cell western blot, and immunofluorescence staining. (A and B) Quantification of (A) collagen I and (B) fibronectin gene expression, normalized to GAPDH expression; (C and D) Quantification of (C) collagen I and (D) fibronectin protein levels, normalized to  $\beta$ -tubulin levels; (E) Cell culture supernatants were collected and tested for hydroxyproline content. (F–G) Immunofluorescence staining for (F) collagen I and (G) fibronectin in KFs. Magnification: 200 $\times$ . (mean  $\pm$  SD,  $n = 3$ , Student  $t$ -test, \* $p < 0.05$ , \*\* $p < 0.01$ , compared with the indicated NF-conditioned medium-treated cells).

various growth factors or cytokines, may responsible for this inhibitor effect and indicate that transplantation of hBMSCs may be an alternative therapeutic strategy for treating hypertrophic scars and keloids.

Skin wound healing is a complex process that requires coordination of a cascade of cellular responses to injury and includes three overlapping stages: the inflammatory phase, the fibroproliferative phase, and the remodeling phase [24]. During the fibroproliferative stage, dermal fibroblasts from the wound margin proliferate and migrate into the wound, generate granulation tissue, and begin to remodel the wound matrix to create new dermal tissue. Many recent studies hypothesize that MSCs exhibit a number of trophic functions that enhance tissue regeneration, such as modulation of dermal fibroblast function and production of antifibrotic factors [7]. Proliferation and migration of dermal fibroblasts also constitute essential steps in the scarring process, with these fibroblasts considered research targets in many studies. Here, we found that BMSC-conditioned medium inhibited cell proliferation and migration in HSFs and KFs, but did not induce apoptosis. In contrast, NF-conditioned medium did not affect HSF or KF proliferation or migration. These data are consistent with a recent study demonstrating that human WJ-MSC-conditioned medium and lysate inhibited the growth of human KFs, with a reduction in cluster-of-differentiation and tumor-associated fibroblast marker expression and migration, interruption of the cell cycle, and inhibition of migration in scratch-wound assays [23].

Compared with this report, we used hBMSCs, a more accessible source of stem cells, to treat the KFs and HSFs and achieved some similar conclusions. However, in another culture condition, the WJ-MSC-conditioned medium enhanced human keloid fibroblasts and normal skin fibroblast proliferation and migration [25]. These inconsistent findings may be a result of the use of different cell culture models and different fibroblast sources.

In the present study, we observed that HSFs and KFs express TGF- $\beta_1$ , TGF- $\beta_2$ , CTGF, and PAI-1 at high transcriptional and translational levels as compared to NFs and MSFs. These overexpressed profibrotic genes are associated with fibrotic disease pathogenesis. TGF- $\beta_1$  and TGF- $\beta_2$  are key pathological inducers of excessive scar formation and may be potential targets for scar reduction therapy [26], given that TGF- $\beta$  overproduction has been implicated in many fibrotic diseases, such as pulmonary fibrosis, intestinal fibrosis, liver cirrhosis, glomerulonephritis, and scleroderma [27,28]. CTGF is a fibrotic marker that mediates fibrotic response to TGF- $\beta_1$  and stimulates fibroblast proliferation and the production of ECM proteins, such as collagen and fibronectin [29]. PAI-1 plays a pivotal role in tissue fibrosis [30] with elevated PAI-1 levels causally linked to elevated collagen synthesis in both NFs and KFs [31]. Most importantly, after 48-h treatment with BMSC-conditioned medium, expression levels of TGF- $\beta_1$ , TGF- $\beta_2$ , CTGF, and PAI-1 were lower in HSFs and especially in KFs. The behavior of fibroblasts, particularly those with a proliferative and profibrotic phenotype, can be altered by MSCs or other cell types through

paracrine signaling [32,33]. Accumulating evidence suggests that paracrine signaling is one of the main underlying mechanisms behind the therapeutic effects of MSCs [17–19]. The expression profile of these profibrotic and antifibrotic genes was also confirmed at the translational level by immunofluorescence staining. In contrast, TGF- $\beta_3$  and decorin, which reportedly prevent fibrosis [34,35], exhibited increased levels of expression at the gene and protein levels in our model. Given that WJ-MSCs decrease TGF- $\beta_3$  gene expression in keloid fibroblasts [25], it is conceivable that WJ-MSCs, which represent a fetal MSC source, involve a more scar-free secretome than that observed in BMSCs, and that this secretome might have different effects on the profibrotic phenotype of keloid fibroblasts. Here, our data indicate that a BMSC-conditioned medium attenuated the fibrotic phenotype of HSFs and KFs through a paracrine signaling mechanism.

We also observed that BMSC-conditioned medium decreased ECM synthesis in HSFs and KFs. This was indicated by decreased expression of collagen I and fibronectin at the gene and protein levels, and low culture supernatant concentrations of hydroxyproline, which is a major component of collagen. A potential alternative interpretation for this phenomenon is that some trophic or immunomodulatory factors of the secretome derived from BMSCs inhibited HSF and KF proliferation, decreased expression of profibrotic factors, and increased expression of antifibrotic factors, which resulted in ECM synthesis. Atypical fibroblasts that excessively deposit ECM components, especially collagen and fibronectin, are common features of hypertrophic scars and keloids [36].

In our culture conditions, paracrine signaling of hBMSCs inhibited the proliferative and profibrotic phenotypes associated with HSFs and KFs. Furthermore, this paracrine signaling does not induce apoptosis or suppress ECM synthesis, suggesting that hBMSCs may be a new therapeutic candidate for treating hypertrophic scars and keloids. However, more research in this paracrine signaling is required to further reveal the underlying mechanism of this inhibitory effect of hBMSCs on the proliferative and profibrotic phenotype of HSFs and KFs in the following experiment. The next experimental plan is searching out the contributing cytokines in the BMSC-conditioned medium and investigating the in vivo effect of BMSC transplantation on the biological behavior of hypertrophic scars and keloids.

## Conflicts of interest

The authors declare no conflicts of interest.

## Appendix A. Supplementary data

Supplementary data associated with this article can be found, in the online version, at <http://dx.doi.org/10.1016/j.jdermsci.2016.03.003>.

Supplemental Fig. S1. Characterization and differentiation of isolated BMSCs.

(A) Analysis of the phenotype of wild-type BMSCs by flow cytometry. Black histograms represent isotype controls. (B) Differentiation of wild-type BMSCs in osteogenic-differentiation or adipocyte-differentiation media showing the formation of calcium, expression of ALPase and formation of lipid droplet.

## References

- [1] K.A. Bielefeld, S. Amini-Nik, B.A. Alman, Cutaneous wound healing: recruiting developmental pathways for regeneration, *Cell. Mol. Life Sci.* 70 (2013) 2059–2081.
- [2] E.E. Tredget, B. Levi, M.B. Donelan, Biology and principles of scar management and burn reconstruction, *Surg. Clin. North Am.* 94 (2014) 793–815.
- [3] S. Ud-Din, A. Bayat, New insights on keloids, hypertrophic scars, and striae, *Dermatol. Clin.* 32 (2014) 193–209.
- [4] L.J. van den Broek, G.C. Limandjaja, F.B. Niessen, S. Gibbs, Human hypertrophic and keloid scar models: principles, limitations and future challenges from a tissue engineering perspective, *Exp. Dermatol.* (2014).
- [5] R. Bagabir, R.J. Byers, I.H. Chaudhry, W. Muller, R. Paus, A. Bayat, Site-specific immunophenotyping of keloid disease demonstrates immune upregulation and the presence of lymphoid aggregates, *Br. J. Dermatol.* 167 (2012) 1053–1066.
- [6] M.J. Lee, J. Jung, K.H. Na, J.S. Moon, H.J. Lee, J.H. Kim, et al., Anti-fibrotic effect of chorionic plate-derived mesenchymal stem cells isolated from human placenta in a rat model of CCl(4)-injured liver: potential application to the treatment of hepatic diseases, *J. Cell. Biochem.* 111 (2010) 1453–1463.
- [7] W.M. Jackson, L.J. Nesti, R.S. Tuan, Mesenchymal stem cell therapy for attenuation of scar formation during wound healing, *Stem Cell Res. Ther.* 3 (2012) 20.
- [8] M. Teng, Y. Huang, H. Zhang, Application of stems cells in wound healing—an update, *Wound Repair Regen.* 22 (2014) 151–160.
- [9] B. Usunier, M. Benderitter, R. Tamarat, A. Chapel, Management of fibrosis: the mesenchymal stromal cells breakthrough, *Stem Cells Int.* 2014 (2014) 340257.
- [10] M. Mohamadnejad, K. Alimoghaddam, M. Mohyeddin-Bonab, M. Bagheri, M. Bashtar, H. Ghanaati, et al., Phase 1 trial of autologous bone marrow mesenchymal stem cell transplantation in patients with decompensated liver cirrhosis, *Arch. Iran. Med.* 10 (2007) 459–466.
- [11] P. Kharazini, P.M. Hellstrom, B. Noorinayer, F. Farzaneh, K. Aghajani, F. Jafari, et al., Improvement of liver function in liver cirrhosis patients after autologous mesenchymal stem cell injection: a phase I–II clinical trial, *Eur. J. Gastroenterol. Hepatol.* 21 (2009) 1199–1205.
- [12] Z. Zhang, H. Lin, M. Shi, R. Xu, J. Fu, J. Lv, et al., Human umbilical cord mesenchymal stem cells improve liver function and ascites in decompensated liver cirrhosis patients, *J. Gastroenterol. Hepatol.* 27 (Suppl. 2) (2012) 112–120.
- [13] M. Cherubino, J.P. Rubin, N. Miljkovic, A. Kelmendi-Doko, K.G. Marra, Adipose-derived stem cells for wound healing applications, *Ann. Plast. Surg.* 66 (2011) 210–215.
- [14] A.I. Arno, S. Amini-Nik, P.H. Blit, M. Al-Shehab, C. Belo, E. Herer, et al., Human Wharton's jelly mesenchymal stem cells promote skin wound healing through paracrine signaling, *Stem Cell Res. Ther.* 5 (2014) 28.
- [15] W.M. Jackson, L.J. Nesti, R.S. Tuan, Concise review: clinical translation of wound healing therapies based on mesenchymal stem cells, *Stem Cells Transl. Med.* 1 (2012) 44–50.
- [16] E. Mansilla, G.H. Marin, F. Sturla, H.E. Drago, M.A. Gil, E. Salas, et al., Human mesenchymal stem cells are tolerized by mice and improve skin and spinal cord injuries, *Transplant. Proc.* 37 (2005) 292–294.
- [17] A.M. Hocking, N.S. Gibran, Mesenchymal stem cells: paracrine signaling and differentiation during cutaneous wound repair, *Exp. Cell Res.* 316 (2010) 2213–2219.
- [18] G. Ren, X. Chen, F. Dong, W. Li, X. Ren, Y. Zhang, et al., Concise review: mesenchymal stem cells and translational medicine: emerging issues, *Stem Cells Transl. Med.* 1 (2012) 51–58.
- [19] K. Khosrotehrani, Mesenchymal stem cell therapy in skin: why and what for, *Exp. Dermatol.* 22 (2013) 307–310.
- [20] J. Liang, R.L. Huang, Q. Huang, Z. Peng, P.H. Zhang, Z.X. Wu, Adenovirus-mediated human interleukin 24 (MDA-7/IL-24) selectively suppresses proliferation and induces apoptosis in keloid fibroblasts, *Ann. Plast. Surg.* 66 (2011) 660–666.
- [21] C. Zhang, X. Kong, H. Zhou, C. Liu, X. Zhao, X. Zhou, et al., An experimental novel study: angelica sinensis prevents epidural fibrosis in laminectomy rats via downregulation of hydroxyproline, IL-6, and TGF- $\beta$  1, *Evid. Based Complement. Alternat. Med.* 2013 (2013) 291814.
- [22] C.J. Liang, Y.H. Yen, L.Y. Hung, S.H. Wang, C.M. Pu, H.F. Chien, et al., Thalidomide inhibits fibronectin production in TGF- $\alpha$ 1-treated normal and keloid fibroblasts via inhibition of the p38/Smad3 pathway, *Biochem. Pharmacol.* (2013) 1594–1602.
- [23] C.Y. Fong, A. Biswas, A. Subramanian, A. Srinivasan, M. Choolani, A. Bongso, Human keloid cell characterization and inhibition of growth with human Wharton's jelly stem cell extracts, *J. Cell. Biochem.* 115 (2014) 826–838.
- [24] G.C. Gurtner, S. Werner, Y. Barrandon, M.T. Longaker, Wound repair and regeneration, *Nature* 453 (2008) 314–321.
- [25] A.I. Arno, S. Amini-Nik, P.H. Blit, M. Al-Shehab, C. Belo, E. Herer, et al., Effect of human wharton's jelly mesenchymal stem cell paracrine signaling on keloid fibroblasts, *Stem Cells Transl. Med.* 3 (2014) 299–307.
- [26] R.L. Chalmers, The evidence for the role of transforming growth factor-beta in the formation of abnormal scarring, *Int. Wound J.* 8 (2011) 218–223.
- [27] W.A. Border, N.A. Noble, Transforming growth factor beta in tissue fibrosis, *N. Engl. J. Med.* 331 (1994) 1286–1292.
- [28] F. Verrecchia, A. Mauviel, Transforming growth factor-beta and fibrosis, *World J. Gastroenterol.* 13 (2007) 3056–3062.
- [29] C.H. Lee, B. Shah, E.K. Moiola, J.J. Mao, CTGF directs fibroblast differentiation from human mesenchymal stem/stromal cells and defines connective tissue healing in a rodent injury model, *J. Clin. Invest.* 120 (2010) 3340–3349.
- [30] A.K. Ghosh, D.E. Vaughan, PAI-1 in tissue fibrosis, *J. Cell. Physiol.* 227 (2012) 493–507.
- [31] T.L. Tuan, P. Hwu, W. Ho, P. Yiu, R. Chang, A. Wysocki, et al., Adenoviral overexpression and small interfering RNA suppression demonstrate that plasminogen activator inhibitor-1 produces elevated collagen accumulation in normal and keloid fibroblasts, *Am. J. Pathol.* 173 (2008) 1311–1325.

- [32] K.J. Ashcroft, F. Syed, A. Bayat, Site-Specific keloid fibroblasts alter the behaviour of normal skin and normal scar fibroblasts through paracrine signalling, *PLoS One* 8 (2013) e75600.
- [33] N. Murao, K.I. Seino, T. Hayashi, M. Ikeda, E. Funayama, H. Furukawa, et al., Treg-enriched CD4+T cells attenuate collagen synthesis in keloid fibroblasts, *Exp. Dermatol.* 23 (2014) 266–271.
- [34] A. Mukhopadhyay, M.Y. Wong, S.Y. Chan, D.V. Do, A. Khoo, C.T. Ong, et al., Syndecan-2 and decorin: proteoglycans with a difference—implications in keloid pathogenesis, *J. Trauma* 68 (2010) 999–1008.
- [35] D. Honardoust, M. Varkey, K. Hori, J. Ding, H.A. Shankowsky, E.E. Tredget, Small leucine-rich proteoglycans, decorin and fibromodulin, are reduced in postburn hypertrophic scar, *Wound Repair Regen.* 19 (2011) 368–378.
- [36] A. Mukhopadhyay, M.Y. Wong, S.Y. Chan, D.V. Do, A. Khoo, C.T. Ong, et al., Syndecan-2 and decorin: proteoglycans with a difference—implications in keloid pathogenesis, *J. Trauma* 68 (2010) 999–1008.